Article

Cell

TMEM175 Is an Organelle K^+ Channel Regulating Lysosomal Function

Graphical Abstract

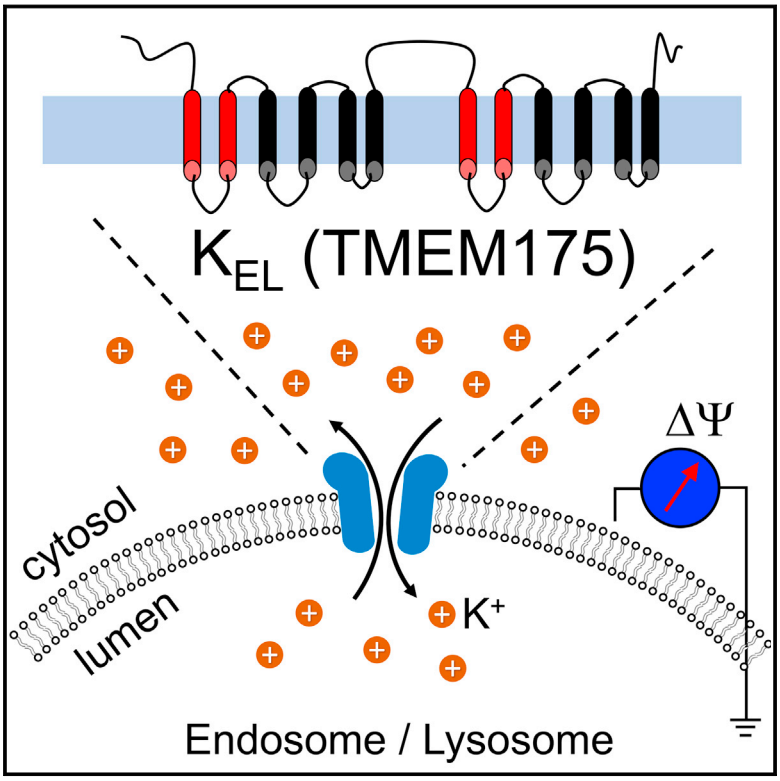

Authors

Chunlei Cang, Kimberly Aranda, Young-jun Seo, Bruno Gasnier, Dejian Ren

Correspondence

dren@sas.upenn.edu

In Brief

Potassium conductance in endosomes and lysosomes is mediated by a channel formed by TMEM175, regulating lysosomal membrane potential, pH stability, and organelle fusion.

Highlights

- Organelle patch clamping recorded a K^+ channel on endosomes and lysosomes
- Candidate gene screening found that a novel protein TMEM175 forms the channel
- TMEM175 regulates lysosomal membrane potential and pH stability
- Knocking out TMEM175 leads to abnormal autophagosome-lysosome fusion

Cang et al., 2015, Cell *162*, 1101–1112
August 27, 2015
http://dx.doi.org/10.1016/j.cell.2015.08.002

CellPress

Article

Cell

TMEM175 Is an Organelle K^+ Channel Regulating Lysosomal Function

Chunlei Cang,[1] Kimberly Aranda,[1] Young-jun Seo,[1] Bruno Gasnier,[2] and Dejian Ren[1,*]
[1]Department of Biology, University of Pennsylvania, 415 South University Avenue, Philadelphia, PA 19104, USA
[2]Paris Descartes University, Sorbonne Paris Cité, Neurophotonics Laboratory, Centre National de la Recherche Scientifique UMR8250, 45 rue des Saints Pères, 75006 Paris, France
*Correspondence: dren@sas.upenn.edu
http://dx.doi.org/10.1016/j.cell.2015.08.002

SUMMARY

Potassium is the most abundant ion to face both plasma and organelle membranes. Extensive research over the past seven decades has characterized how K^+ permeates the plasma membrane to control fundamental processes such as secretion, neuronal communication, and heartbeat. However, how K^+ permeates organelles such as lysosomes and endosomes is unknown. Here, we directly recorded organelle K^+ conductance and discovered a major K^+-selective channel K_{EL} on endosomes and lysosomes. K_{EL} is formed by TMEM175, a protein with unknown function. Unlike any of the ~80 plasma membrane K^+ channels, TMEM175 has two repeats of 6-transmembrane-spanning segments and has no GYG K^+ channel sequence signature-containing, pore-forming P loop. Lysosomes lacking TMEM175 exhibit no K^+ conductance, have a markedly depolarized $\Delta\Psi$ and little sensitivity to changes in $[K^+]$, and have compromised luminal pH stability and abnormal fusion with autophagosomes during autophagy. Thus, TMEM175 comprises a K^+ channel that underlies the molecular mechanism of lysosomal K^+ permeability.

INTRODUCTION

A hallmark of eukaryotic cells is the separation of cellular functions in membrane-bound organelles in the cytosol. Voltage gradients exist across both plasma and organelle membranes. The plasma membrane potential (V_m) regulates cellular processes fundamental to life, including fertilization, gene expression, secretion, neuronal communication, and the beating of cardiac cells. At rest, the plasma membrane is much more permeable to K^+ than to Na^+, leading to a resting V_m closer to the equilibrium potential of K^+ (E_K) (see Hille [2001] for review). K^+ channels represent the largest superfamily of ion-selective channels, with ~80 pore-forming subunit-encoding genes and many more "auxiliary" subunit ones in humans (see Huang and Jan [2014] and Nichols and Lopatin [1997] for review). Despite the divergence in sequence and structure among the ~80 K^+ channels, their ion-selective filters are all formed by similar membrane re-entrant P loops containing the GYG/GFG K^+ channel signature (Doyle et al., 1998; Heginbotham et al., 1994; Jiang et al., 2003; MacKinnon and Miller, 1989; Yellen et al., 1991). In addition to voltage-dependent K^+ channels, there is also a family of voltage- and time-independent "leak" (K2P) K^+ channels (see Goldstein et al. [2001] for review). K2Ps regulate resting background K^+ conductance. Intriguingly, K2Ps are only found in eukaryotes. It is unknown whether the plasma membranes of bacteria and archaea also have "leak-like" K^+ channels.

In lysosomes and endosomes, electrical potential across the organelle membrane ($\Delta\Psi$, defined as $V_{cytosol} - V_{lumen}$; Bertl et al., 1992; Figure 1A) may vary among cells and individual organelles as the organelles mature from early to late endosomes. The ionic conductances determining $\Delta\Psi$ have not been well studied. Earlier indirect studies using the measurement of each ion's ability to influence lysosome luminal pH or to protect the organelles from osmotic lysis suggest that lysosomes are permeable to cations with an approximate permeability sequence of $Cs^+>K^+>>Na^+$ (Casey et al., 1978; Henning, 1975). Recent studies have uncovered several lysosomal ion channels/transporters conducting Cl^-, H^+, Ca^{2+}, and Na^+ (see Xu and Ren [2015]) for review). However, the molecular identity of the large K^+ permeability, its contribution to $\Delta\Psi$, and $\Delta\Psi$'s roles in cellular functions are little understood.

In this report, we discovered a "leak-like" K^+ conductance K_{EL} on endosomes and lysosomes. Using candidate gene screening, we found that TMEM175, a previously uncharacterized family of transmembrane proteins, form K_{EL}. Bacteria and archaea also have TMEM175 homologs that form plasma membrane K^+-permeable channels. Therefore, TMEM175 represents a new K^+ channel family found in all the three domains of life. Unlike plasma membranes, the organelle membrane has little redundancy to K^+ channel proteins; knocking out TMEM175 eliminates the K^+ conductance and leads to compromised organelle lysosomal pH stability and abnormal organelle fusion during autophagy.

RESULTS

A Voltage-Independent K^+ Conductance in Endosomes and Lysosomes

To directly record the K^+ permeability, we used whole-organelle patch clamp to measure the charge flow rates (currents) across lysosomal membranes with K^+ as the major ion (Figure 1A). Similar to those we previously recorded from peritoneal

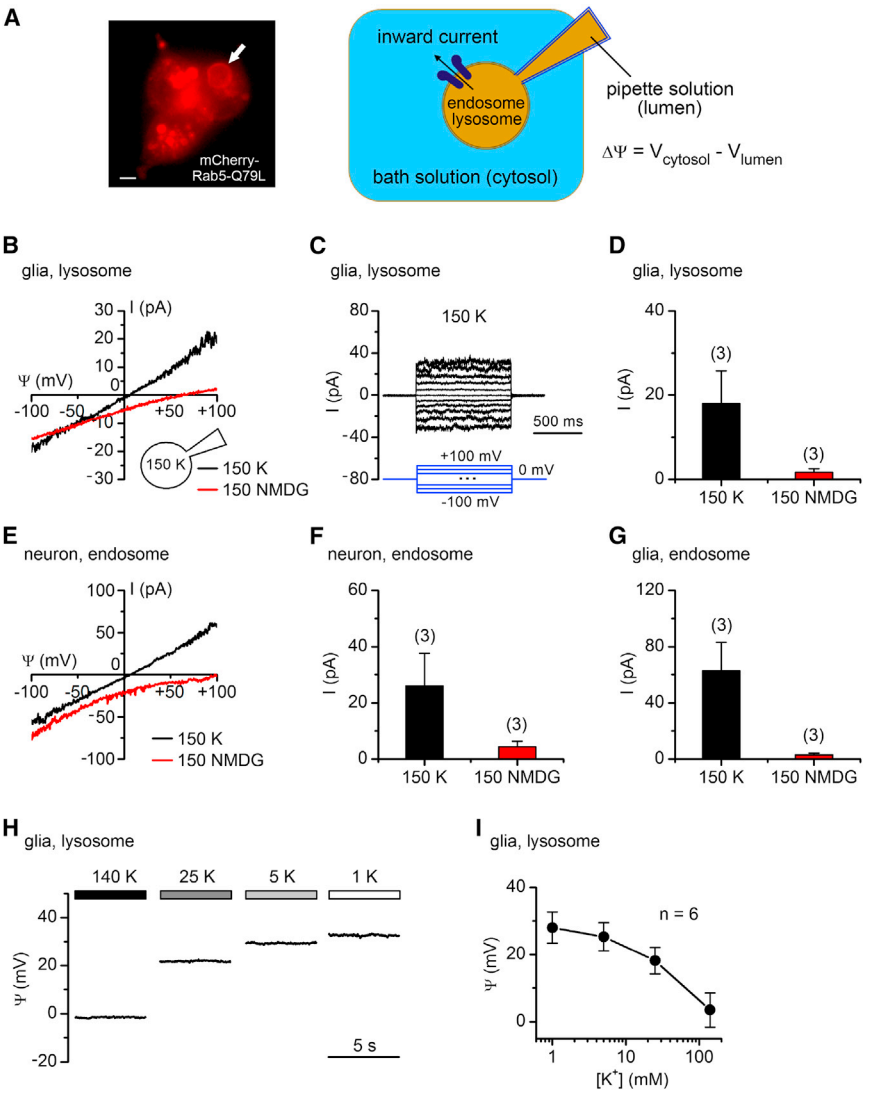

Figure 1. A K^+ Conductance in Endosomes and Lysosomes

(A) Diagrams illustrating the recording techniques and nomenclature used. Endosomes (enlarged by transfecting a mCherry-tagged Rab5-Q79L mutant, illustrated in the left panel with arrow indicating an enlarged one; scale bar, 5 μm) or lysosomes (enlarged with treatment of vacuolin-1) are individually released from each cell sliced open with a glass pipette and are subject to recordings (right). $\Delta\Psi$ (Ψ) is the voltage across organelle membrane with lumen used as the reference (Bertl et al., 1992). Inward cation current (negative) denotes the movement of positive charges out of the organelle lumen into cytosol (bath).

(B–G) Currents recorded under voltage-clamp from lysosomes (B–D) and endosomes (E–G) of cultured mouse glia (B–D and G) and neurons (E and F). Pipette solution contained 150 mM K^+. Bath contained 150 mM K^+ (symmetrical [K^+] condition) or 150 mM NMDG (non-symmetrical) as indicated. In (B) and (E), ramp voltage protocols (−100 to +100 mV in 1 s, Vh = 0 mV) were used to record the currents. In (C), step protocols (−100 to +100 mV with a 20 mV step, illustrated) were applied under symmetrical [K^+] condition. Column figures (D, F, and G) summarize the current amplitudes at +100 mV recorded with ramp protocols.

(H and I) Lysosomal membrane potential (Ψ) recorded under current-clamp (I = 0). (H) Representative traces recorded under varying bath (cytosolic) [K^+]. (I) Averaged Ψ values. Numbers of organelles recorded are in parentheses. Data are presented as mean ± SEM.

See also Figure S1.

macrophages (Cang et al., 2014), lysosomes from primary cells cultured from mice, including glia (Figures 1B–1D), neurons, cardiac myocytes, and cardiac fibroblasts (Figure S1), all had high densities (~50 pA/pF at +100 mV) of K^+ currents.

On plasma membranes, there is a large degree of heterogeneity in the kinetics of activation, inactivation, and deactivation in the K^+ conductances (Hille, 2001). Such heterogeneity appeared to be absent or minimal in lysosomes recorded from both excitable and non-excitable cells. In response to changes in voltage, the current amplitudes changed instantaneously, were proportional to the applied voltages, and had no obvious inactivation or rectification, properties of a voltage- and time-independent, leak-like K^+ channel conductance (Figures 1C and S1).

To test whether similar K^+ conductance is present in other intracellular organelles, we patch clamped endosomes (Saito et al., 2007). To facilitate whole-organelle recording, we enlarged the endosomes with transfection of Rab5-Q79L, a Rab5 mutant that enlarges endosomes (Stenmark et al., 1994). In endosomes tested in all the cell types cultured from mice, including neurons (Figures 1E and 1F), glia (Figure 1G) and cell lines, we detected K^+ currents with properties similar to those found in lysosomes.

These results indicate that both endosomes and lysosomes have a leak-like K^+ conductance (K_{EL}), which presumably underlies the K^+ permeability. Consistent with the idea that K_{EL} is constitutively open, the resting $\Delta\Psi$ of lysosomes, like that of V_m, was highly dependent on [K^+] (Figures 1H and 1I).

A Candidate Gene Screening to Identify K_{EL}

We set out to identify the K_{EL}-encoding gene. Among the ~80 canonical K^+ channels characterized on plasma membranes, only the K2P family has biophysical properties that resemble K_{EL} (Goldstein et al., 2001). K2P1 protein has been detected in endosomes using immunostaining (Honoré, 2007). Overexpressing K2P1 in HEK293T cells, however, led to no obvious increase in K_{EL}-like currents recorded from endosomes (enlarged with Rab5-Q79L) or lysosomes (enlarged with vacuolin-1) (n = 15).

We next used a whole-organelle patch-clamp-based candidate gene screening to test whether previously under-characterized proteins form K_{EL}. We used the following candidate selection criteria: (1) the protein was found in our previous lysosomal

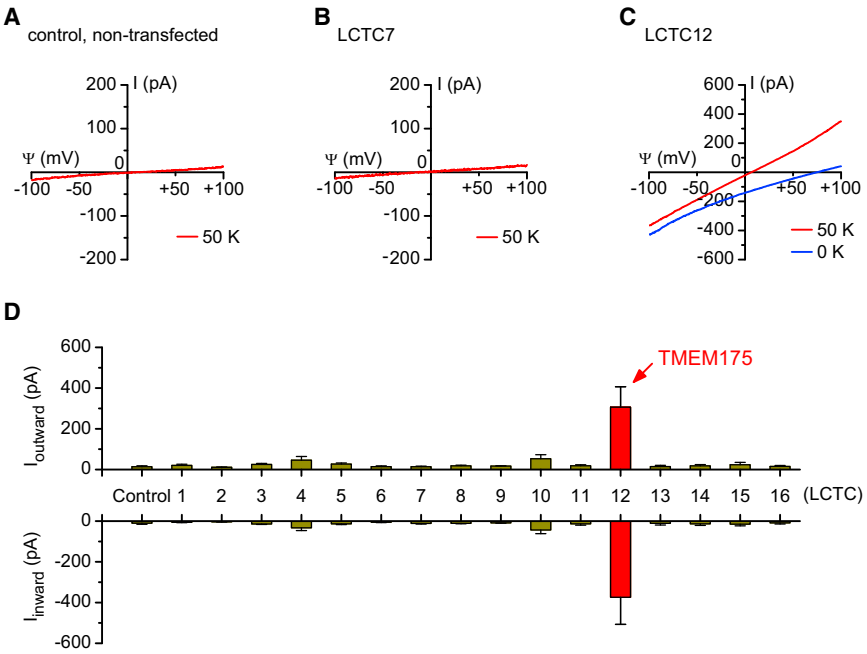

Figure 2. Identification of K_{EL} Using Candidate Gene Screening

Lysosomal currents were recorded from HEK293T cells transfected with lysosomal channel/transporter candidates (LCTC1–16).

(A–C) Representative currents recorded from non-transfected cells (A, control) and cells transfected with LCTC7 (B) or with LCTC12 (C).

(D) Averaged amplitudes of outward (at +100 mV; top) and inward (at −100 mV; bottom) currents from cells transfected with each of the 16 candidates. n = 4 to 7. A ramp protocol (−100 mV to +100 mV) was used. The 16 candidates (LCTC1–16) tested are (in order) CLN3, CLN7, rPQLC2, TMEM104, SLC38A7, TTYH2, PTTG1IP, TTYH3, MFSD1, SLC37A2, SLC46A3, TMEM175, CLN5, CLN6, CLN8, and TMEM127, all from human except rPQLC2 (from rat). Data are presented as mean ± SEM.

proteomic analysis (Chapel et al., 2013) or is known to lead to lysosome-related disease when mutated; (2) the protein is predicted to have at least one transmembrane spanning (TM) domain; and (3) the protein has not been functionally established as an ion channel/transporter. Because of the small size (~−80 pA at −100 mV in HEK293T cell lysosomes) of the native K_{EL} current (I_{KEL}) and potential genetic redundancy, a loss-of-function approach with shRNAs to partially knockdown candidate proteins might not be sufficiently sensitive for the screening. We instead used a gain-of-function approach by testing whether overexpression of candidate proteins increased lysosomal currents. To screen proteins for channel current, we performed recordings under conditions that detected K^+, Na^+, and Cl^- currents. We also included amino acids in the pipette solution to detect amino-acid-activated conductance. Out of the 16 candidates, 12 of which were detected in our previous proteomic analysis (Chapel et al., 2013), only 1 (TMEM175) led to a large increase of I_{KEL}-like currents (Figure 2).

TMEM175 Is a Novel Protein in Both Endosomes and Lysosomes

TMEM175 (transmembrane protein 175) has no significant sequence similarity to any other protein with known function. Homologs are found in archaea, bacteria, and eukaryotes and are grouped together into a superfamily by the presence of one (in archaea and bacteria) or two (in eukaryotes) copies of DUF1211 (domain-of-unknown-function). Within eukaryotes, TMEM175 is found in both unicellular organisms such as the choanoflagellate *Salpingoeca rosetta* (Genbank: XP_004995857) and marine microalgae *Nannochloropsis gaditana* (EWM26717) and multicellular organisms, including invertebrate and vertebrate animals. Among animals, TMEM175s are highly conserved (81% identity between human and mouse, 62% between human and zebrafish). Expressed-sequence-tag and RNA-sequencing databases suggest that human TMEM175 (hTMEM175) is expressed in all tissues/organs, including the heart, brain, testis, kidney, and liver, and in cultured cell lines.

Using hydrophobicity analysis (Figure 3A) and a hidden Markov model method (Tusnády and Simon, 2001), hTMEM175 is predicted to have a two-repeat structure, with each repeat containing six TMs (S1–S6, Figure S2A). The two repeats have significant sequence similarity (Figure S2B), especially in the first TMs (IS1 and IIS1). This 2 × 6TM structure is similar to that of the two-repeat Na^+ channels TPCs (Zhu et al., 2010). TMEM175's S4s have no obvious voltage-sensing domains characterized by the presence of charged residues, unlike in K_Vs, Na_Vs, Ca_Vs, and TPCs. Intriguingly, the predicted S5–S6 linkers in both the repeats are short (4 aa). A GYG/GFG-signature-containing P loop (Figure S2A), a linker that reenters the membrane to form the selectivity filter of all the known K^+ channels, is lacking (MacKinnon and Miller, 1989; Miller, 1995). Using an accessible-cavity geometry-based set of criteria (Pore-Walker) (Nugent and Jones, 2012), IS1, IIS1, and IIS2 are predicted to potentially contain channel pore-lining helices.

TMEM175 was previously detected from lysosomal membrane protein preparations by mass spectrometry (Chapel et al., 2013; Schröder et al., 2007). To elucidate the localization of TMEM175, we tagged hTMEM175 with fluorescence proteins at its N terminus (with EYFP) or C terminus (with EGFP) (Figure 3B). The tagged TMEM175 partially colocalized with endosomal (Rab5, Figures 3C and 3E) and lysosomal (Lamp1, Figures 3D and 3F; Chapel et al., 2013) markers. Because GFP and YFP lose fluorescence at acidic pH found in the lumen of lysosomes, the detection of bright YFP and GFP signals overlapping with Lamp1 suggests that the N and C termini of TMEM175 are localized in the cytosol (Figure 3A), a topology similar to that of TPCs (Zhu et al., 2010).

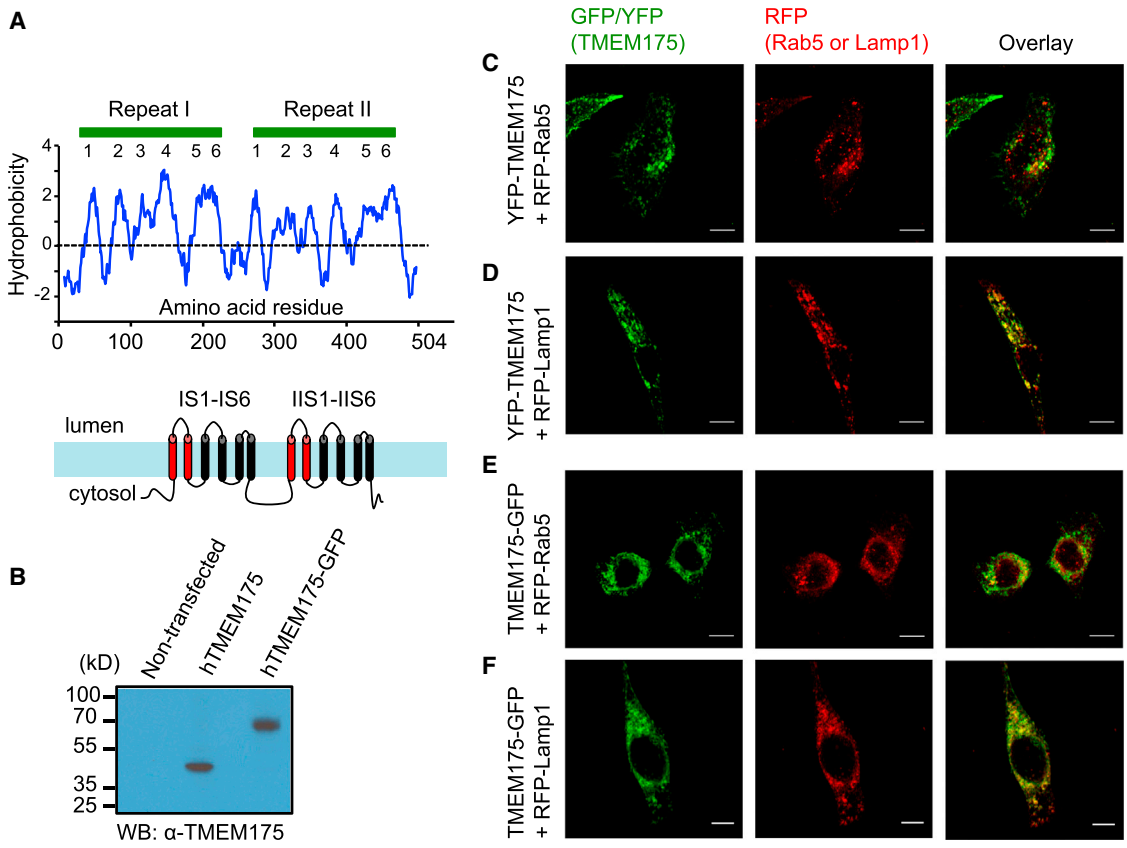

Figure 3. TMEM175 Is Expressed in Endosomes and Lysosomes

(A) Top: hydrophobicity plot of human TMEM175 (hTMEM175). Bottom: a predicted two-repeat six-transmembrane-spanning (2 × 6TM) topology of hTMEM175. Domains that may contain the pore lining are in red.

(B) Western blot detecting non-tagged and GFP-tagged hTMEM175 transfected in HEK293T cells.

(C and D) Localization of N-terminally YFP-tagged hTMEM175 with RFP-tagged Rab5 (C) or RFP-tagged Lamp1 (D) co-transfected in HeLa cells.

(E and F) Co-localization of C-terminally GFP-tagged hTMEM175 with RFP-tagged Rab5 (E) or RFP-tagged Lamp1 (F). Scale bars, 5 μm.

See also Figure S2.

TMEM175 Forms K_{EL} Channels on Endosomes and Lysosomes

We transfected HEK293T cells with YFP-tagged hTMEM175 to identify TMEM175-expressing organelles to use for patch clamping. Overexpressing hTMEM175 led to large K^+ currents in both endosomes (438.5 ± 133.5 pA/pF at +100 mV; n = 13; Figures 4A–4F) and lysosomes (374.3 ± 96.8 pA/pF, n = 6; Figures 4G–4I). Like the native I_{KEL}, TMEM175 currents ($I_{TMEM175}$) rose and fell instantaneously upon voltage changes without rectification (Figures 4E and 4H). Unlike K_Vs, TMEM175 did not inactivate even when tested with pulses of 10 s duration (Figure S3A).

TMEM175 Is K^+ Selective

Removing K^+ from the bath containing Cl^- abolished the current, indicating that hTMEM175 is not permeable to anions (Figure 5A). The current increased when K^+ was replaced with Rb^+, suggesting that, like many canonical K^+ channels, hTMEM175 is Rb^+ permeable (Figure 5A). To determine hTMEM175's cation selectivity, we recorded $I_{TMEM175}$ under various ionic conditions. Replacing bath K^+ with NMDG, Na^+, or Ca^{2+} largely abolished the outward currents (moving into lysosomes) (Figures 5A–5C), suggesting that hTMEM175 is minimally permeable to NMDG, Na^+ and Ca^{2+}. We recorded $I_{hTMEM175}$ under bi-ionic conditions and used the resulting reversal potentials to quantify hTMEM175's relative permeability (Figures 5D and 5E). hTMEM175 was selective for K^+ over Na^+ and Ca^{2+} (P_K/P_{Na} = 36.0 ± 4.4, n = 11; P_K/P_{Ca} = 141.6 ± 27.7, n = 9), with a P_K/P_{Na} within the range of those of K_V and K_{2P} channels (Heginbotham et al., 1994; Honoré, 2007). Unlike the canonical K^+ channels but similar to the behavior of lysosomal membranes (Casey et al., 1978; Henning, 1975), hTMEM175 permeated Cs^+ better than K^+ (Figure 5B; P_K/P_{Cs} = 0.51 ± 0.03, n = 9).

We tested whether K^+ conduction through hTMEM175 required a co-movement of H^+, a property of H^+ cotransporter/exchangers. Under conditions where there was no H^+ gradient (pH_{lumen} = $pH_{cytosol}$ = 7.2) and K^+ was the only other permeable cation, the reversal potential follows the changes in $[K^+]_{cyt}$ with a slope of 56.8 mV/decade (Figure 5F), close to that of a pure K^+ electrode (58.8 mV/decade at 23°C), suggesting that H^+ co-movement is not required (Accardi and Miller, 2004).

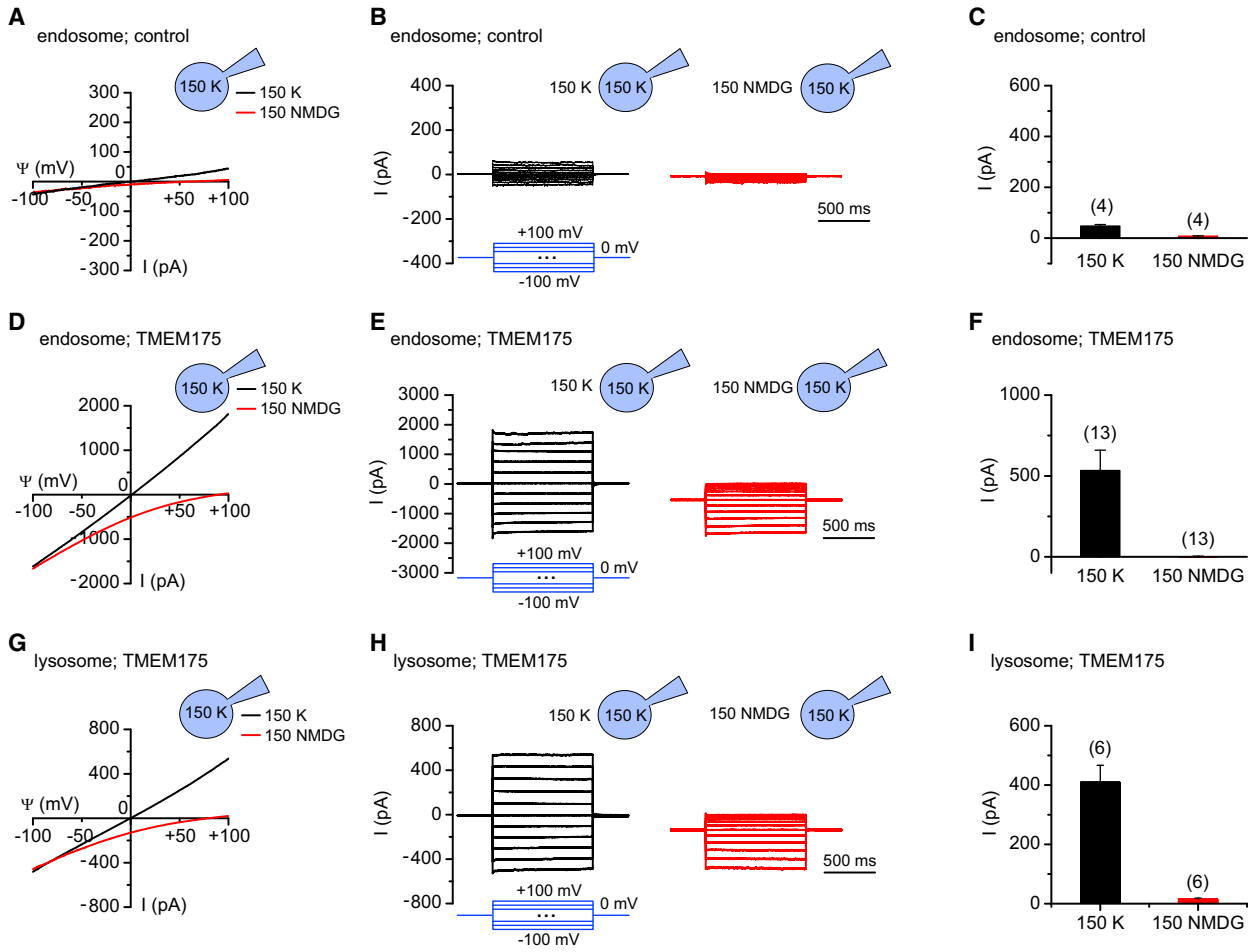

Figure 4. TMEM175 Forms a Voltage-Independent, Non-Inactivating Channel

(A–I) Whole-endosomal (A–F) and lysosomal (G–I) currents recorded from non-transfected (A–C) or hTMEM175-transfected (D–I) HEK293T cells. Representative current traces recorded using a ramp protocol (A, D, and G: −100 to +100 mV in 1 s, Vh = 0 mV) or step pulses (B, E, and H: −100 to +100 mV, 20 mV step, Vh = 0 mV, illustrated) under conditions of symmetrical [K^+] (150 mM in both lumen and cytosol; black lines) or non-symmetrical [K^+] (150 mM K^+ in lumen and 150 mM NMDG in cytosol; red lines) conditions are shown. (C, F, and I) Averaged current amplitudes at +100 mV obtained with the ramp protocol. Non-transfected cells had little lysosomal currents (see Figure 2A). Data are presented as mean ± SEM. See also Figure S3.

The Conserved *FSD* Signature Is Required for TMEM175 Function

The highest sequence similarity among TMEM175s is found in IS1 and IIS1. These two regions contain an *FSD* signature conserved in TMEM175s of eukaryotes (Figure S2A), bacteria, and archaea. TMEM175 with the *FSD* signature mutated generated proteins comparable to that of the wild-type (WT; as judged by the intensity of the attached YFP protein, data not shown). However, the mutants exhibited no active channel activity (Figures S3B and S3C).

TMEM175 Has Pharmacological Properties Distinct from Those of Canonical K^+ Channels

$I_{TMEM175}$ was not inhibited by Cs^+, Ba^{2+}, tetraethylammonium, or quinine at concentrations commonly used to block canonical K^+ channels but was sensitive to Zn^{2+} (IC_{50}, 38.4 μM) and 4-aminopyridine (4-AP; IC_{50}, 35.0 μM) (Figures S3D–S3G). The lack of voltage dependence and the distinct pharmacological properties suggest that $I_{TMEM175}$ was not the result of a potential upregulation of canonical K^+ channel proteins caused by overexpressing TMEM175.

Bacterial TMEM175 Homologs with Only One Repeat Form Plasma Membrane Voltage-Independent K^+-Permeable Channels

The predicted 2 × 6TM structure of hTMEM175 is similar to that of the TPC channels but deviates from those of most other ion channels whose structures are 2TMs, 6TMs, or 4 × 6TM. To test whether proteins with only one of the two repeats can form ion channels, we expressed the bacterial TMEM175 homologs (bacTMEM175s) from gram-positive (Chryseobacterium; Genbank: KFF73457; cbTMEM175) and gram-negative (*Streptomyces collinus*, Genbank: AGS72644; scTMEM175) bacteria in HEK293T cells.

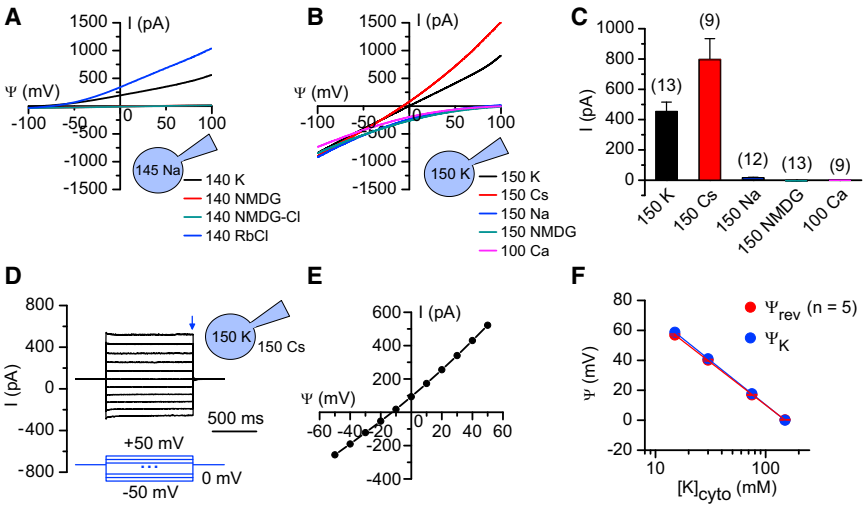

Figure 5. TMEM175 Is K^+ Selective

(A and B) Representative endosomal currents recorded using a ramp protocol (−100 to +100 mV in 1 s, Vh = 0 mV) from hTMEM175-transfected HEK293T cells with pipette (lumen) solutions of 145 mM Na^+ (A) or 150 mM K^+ (B) and bath (cytosol) solutions containing various cations (concentrations indicated). The green (for NMDG-Cl) and red (for NMDG) traces in (A) overlap and are not well separated.

(C) Current amplitudes measured at +100 mV of the ramp protocol used in (B).

(D) Representative current traces elicited by step pulses from −50 to +50 mV (10 mV step) under bi-ionic conditions (150 mM K^+ in lumen and 150 ms Cs in cytosol).

(E) Current amplitudes measured at the end of the steps in (D) (indicated by arrow) were plotted against the test voltages to determine the reversal potential.

(F) Reversal potentials (Ψ_{rev}) recorded with a 150 mM K^+-containing pipette solution and cytosol solutions containing 150, 75, 30, or 15 mM $[K^+]$. Ψ_K, K^+ equilibrium potential. Data are presented as mean ± SEM.

The prokaryotic TMEM175s are small (192 aa in cbTMEM175 and 206 aa in scTMEM175) and are predicted to have only one 6TM repeat (Figure 6A). Bacterial and human TMEM175s are conserved, especially in the first two TMs (cbTMEM175 versus hTMEM175 repeat II: 39% identity, 56% similarity; Figures S4A–S4D). As a reference, the mammalian protein with the highest similarity to the bacterial Na^+ channel NaChBac is the 4 × 6TM T-type Ca^{2+} channel $Ca_V3.1$. The identity and similarity between $Ca_V3.1$ and NaChBac are 27% and 51%, respectively.

Unlike most other bacterial ion channel proteins, bacTMEM175s were readily expressed in mammalian cells. HEK293T transfected with bacTMEM175s had large K^+ currents when recorded under symmetric $[K^+]$ conditions (Figures 6, S4F, and S4G). Thus, prokaryotes use TMEM175 homologs, instead of K2Ps, to form K^+-permeable leak-like channels. As bacteria and archaea have no intracellular organelles, the function of TMEM175 is perhaps to set the membrane potentials of the cells and/or to regulate cellular osmolarity.

The sequence similarity between the two bacTMEM175s (35% identity, 59% similarity) is only as large as the similarity between each and hTMEM175 (Figure S4). The two, however, generated currents with similar properties. Like hTMEM175, bacTMEM175s also had linear current (I)-voltage (V) relationships and the currents did not inactivate (Figures 6D, 6E, and S4F). Compared to hTMEM175, bacTMEM175s were less permeable to Cs (P_K/P_{Cs}: 2.1 ± 0.7, n = 4 for cbTMEM175; 2.3 ± 0.3, n = 5 for scTMEM175) and were noticeably permeable to Na^+ (P_K/P_{Na}: 2.4 ± 0.5, n = 4 for cbTMEM175; 4.4 ± 1.4, n = 5 for scTMEM175). Unlike hTMEM175, bacTMEM175s were not inhibited by 4-AP when applied either in the bath or in the pipette solutions (Figures 6G and S4H). The distinction in ionic selectivities and channel blocker sensitivity of conductance generated from different TMEM175 proteins support the idea that TMEM175 forms the ion conductive pore that determines ion selectivity.

TMEM175 Is the Major Lysosomal K^+ Conductance

To determine the extent to which TMEM175 contributes to the total K^+ conductance in lysosomes, we used the CRISPR/Cas9 technique to knock out mouse TMEM175 (mTMEM175) in RAW264.7, a leukemic monocyte macrophage cell line commonly used for lysosomal studies (Steinberg et al., 2010). We selected PAM-adjacent sequences encoding the second putative TM (IS2) to target such that channel function would be disrupted by both frame-shifting indels resulting in protein truncation and by non-frame-shifting indels resulting in rotation of the membrane-spanning α-helix (Figure 7A). For the control of specificity, we used a CRISPR construct that targets hTMEM175 but does not match mTMEM175 sequences. Knocking out mTMEM175 eliminated I_{KEL} (Figures 7B, 7C, and 7E). As an additional control, transfecting hTMEM175 cDNA into the mouse knockout cells rescued and enhanced I_{KEL} (Figures 7D and 7E).

To further rule out the possibility that the elimination of I_{KEL} in the CRISPR KO cells resulted from off-targeting by the synthetic guide RNA at the genomic level, we also used short hairpin interfering RNAs (shRNAs) to knock down mTMEM175 in RAW264.7 cells and hTMEM175 in HEK293T cells. Transfecting targeting shRNAs markedly reduced the native I_{KEL} (Figure S5). Together, the knockout and knockdown experiments suggest that TMEM175 is required for K_{EL} and that other channels contribute little to the K^+ conductance. We conclude that K_{EL} results from TMEM175 (hereafter called K_{EL}).

K_{EL} Determines ΔΨ and Its Sensitivity to K^+

To determine the function of the dominant organelle K^+ conductance, we performed current-clamp recordings to test whether K_{EL} controls ΔΨ. Similar to those from glia (Figure 1I) and peritoneal macrophages (Cang et al., 2013), artificially enlarged lysosomes from RAW264.7 cells under the whole-organelle patch clamp configuration had a positive "resting" membrane potential (lumen more negative than cytosol) when $[K^+]_{cyt}$ was 140 mM, close to its physiological concentration (Figure 7H).

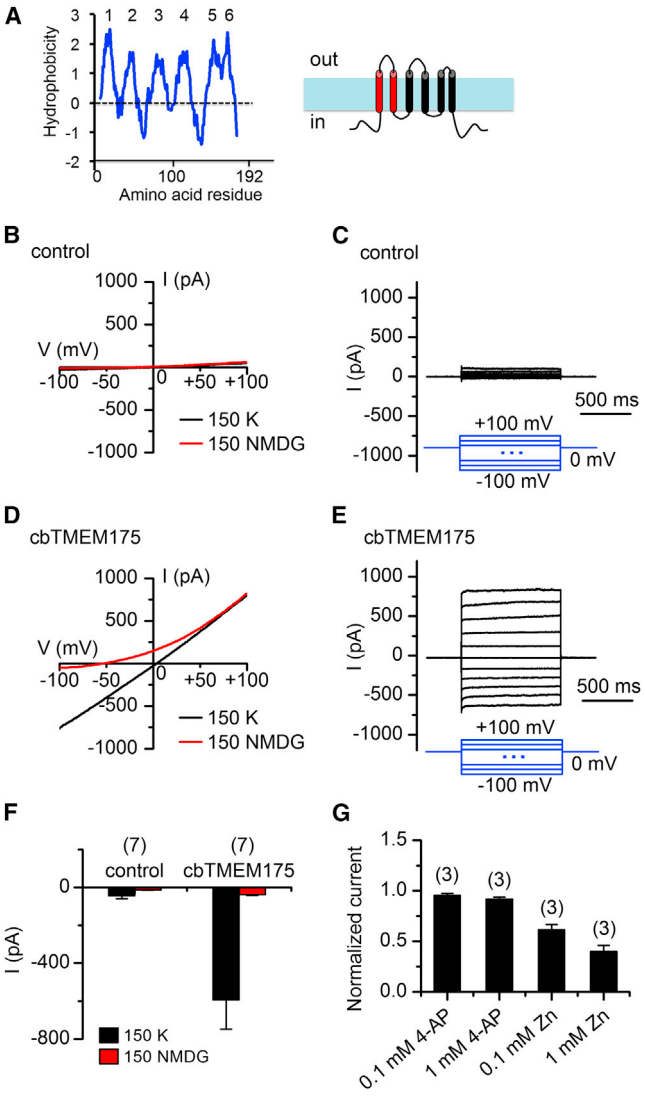

Figure 6. Bacterial TMEM175 Homologs Form K^+-Permeable Channels

(A) Hydrophobicity plot (left) and a predicted one-repeat 6TM structure (right) of a bacterial TMEM175 from Chryseobacterium (cbTMEM175).

(B–E) Representative whole-cell plasma membrane currents recorded from control (mock-transfected, B and C) HEK293T cells and cells transfected with the cbTMEM175 (D and E) using ramp protocols (B and D; −100 mV to +100 mV in 1 s, Vh = 0 mV) or step protocols (C and E) as illustrated.

(F) Averaged current amplitudes at −100 mV with bath cation concentrations indicated.

(G) Drug sensitivity presented as the current amplitudes (at −100 mV) after drug application, normalized to the amplitudes before drug application. Numbers of cells recorded are in parentheses. Data are presented as mean ± SEM.

See also Figure S4.

Compared to WT, lysosomes from the K_{EL} knockout cells were 14 mV depolarized. When $[K^+]_{cyt}$ was reduced to 1 mM, a condition under which a K^+ conductance presumably generates depolarization, the KO lysosomes were 23 mV hyperpolarized compared to WT (Figure 7H).

$\Delta\Psi$ versus $[K^+]_{cyt}$ shows that lysosome potential was directly correlated with K^+ in the WT. Strikingly, the K^+ sensitivity was essentially absent in the KO lysosomes (Figures 7F–7H). Thus, K_{EL} controls lysosomal $\Delta\Psi$ and is the major determinant of $\Delta\Psi$'s sensitivity to K^+.

K_{EL} Contributes to Lysosomal pH Stability

In addition to setting $\Delta\Psi$, K^+ may also serve as a counterion to maintain the acidic pH in the lumen (Haggie and Verkman, 2009; Mindell, 2012; Steinberg et al., 2010). Under nutrient-replete conditions, lysosomes in the RAW264.7 KO cells exhibited pH close to that in the WT cells. When cells were starved for 2 hr, the KO lysosomes became alkalinized by 0.7 units to 5.3, while the WT maintained their pH of 4.8 (Figures 7I–7K). Thus, K_{EL} contributes to lysosomal pH stability.

K_{EL} Regulates Organelle Fusion

Because of the charges of lipids and proteins on the membrane, a function of $\Delta\Psi$ may be to regulate the organelle's fusion with other organelles. We tested K_{EL}'s potential role in organelle fusion by comparing the autophagosome-lysosome fusion in the WT and KO cells. During starvation, cells generate autophagosomes that fuse with lysosomes to deliver engulfed materials for digestion and recycling (see Mizushima and Komatsu [2011] for review). We used LC3 (microtubule-associated proteins 1A/1B light chain 3A) tandem tagged with mCherry and GFP (RFP-GFP-LC3) as an autophagosome marker to monitor the numbers of autophagosomes before (RFP- and GFP-positive puncta) and after (RFP positive, but GFP negative because of low GFP activity at acidic pH in lysosomes) fusion with lysosomes (Cang et al., 2013; Klionsky et al., 2012). The total number of autophagosomes formed during 2 hr of starvation was similar in the WT and the KO cells (Figures 7L and 7M), indicating that the formation of autophagosomes as an early step of autophagy does not require K_{EL}. However, the number of GFP-positive puncta (Figures 7L and 7M) and the ratio of numbers of GFP-positive to RFP-positive puncta (Figure 7N) were significantly lower in the KO, suggesting accelerated fusion of the autophagosomes to lysosomes, presumably due to depolarization of the KO lysosomes. As a control, the numbers of GFP-positive puncta were similar in the WT and KO when cells were incubated with bafilomycin to suppress the autophagosome-lysosome fusion (Klionsky et al., 2012). Furthermore, transfecting hTMEM175 into the KO cells restored the number of GFP-positive puncta (Figures 7L–7N).

DISCUSSION

We have uncovered the mechanism of endosomal and lysosomal K^+ permeability. K_{EL} has a structure drastically different from the canonical K^+ channels in both the number of TMs and the formation of pore region. K_{EL} determines $\Delta\Psi$'s sensitivity to K^+ and is the major control for $\Delta\Psi$, which regulates lysosomal pH stability and organelle fusion. Together with the extensive studies of plasma membranes K^+ conductances in the past seven decades, how the most abundant intracellular ion, K^+, permeates both plasma and the intracellular organelle membranes has now been revealed at the molecular level.

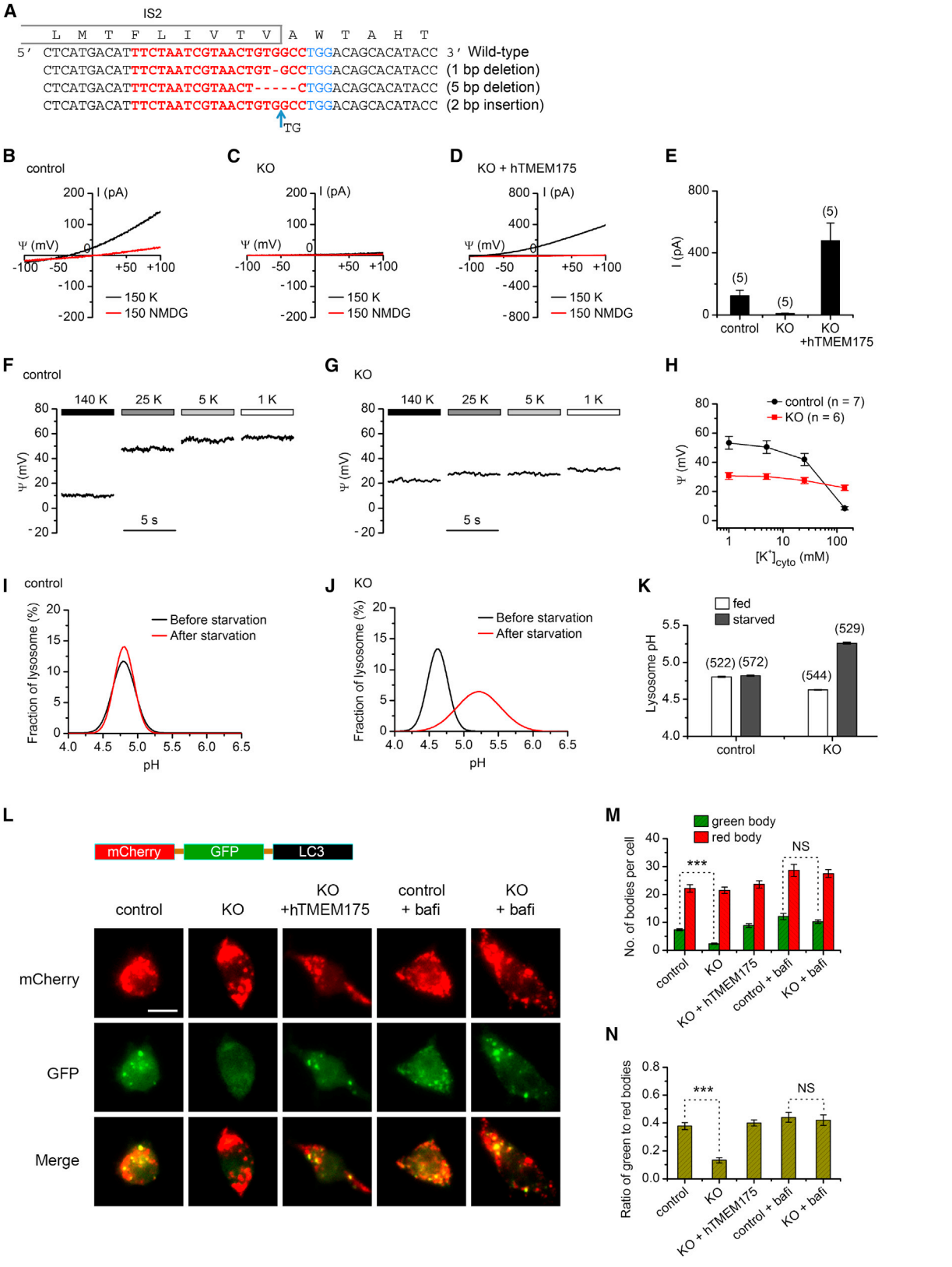

(legend on next page)

Is TMEM175 an ion-conducting subunit of K_{EL} or an "auxiliary" subunit of a pore-forming protein yet to be identified? Multiple lines of evidences suggest that TMEM175 forms the ion conduction pathway. First, the properties of K_{EL} conductance are consistent with the idea that TMEM175 is an ion channel. At ~1 nS (~−100 pA at −100 mV) on a membrane area of $\sim 10^{-7}$ cm^2 (assuming ~3 μm diameter of the enlarged lysosome; 1 pF capacitance), the native total organelle K_{EL} conductance is remarkably high and is comparable to that of many ion channels such as K_Vs and Na_Vs found abundantly in the plasma membrane of excitable cells. For a membrane with 1,000 functional K_{EL} channels, the single K_{EL} conductance would need to be 1 pS even if K_{EL} functions as a constantly open channel (P_o = 1.0). This single-channel conductance is within the range of those of many ion channels and higher than the ~fS value found in the CRAC and Kir7.1 channels (Krapivinsky et al., 1998; Zweifach and Lewis, 1993). In addition, overexpressing TMEM175 in HEK293T cell lysosomes drastically increased I_{KEL} to as large as ~1 nA (~3.5 mA per cm^2 surface area) at −100 mV, a conductance of ~35 mS/cm^2. Furthermore, I_{KEL} doesn't require ATP or other ions, a property generally found in ion channels but distinct from those of transporters. Second, knocking out TMEM175 abolished I_{KEL}. Auxiliary subunits may regulate the channel's biophysical properties but knocking them out usually does not abolish the currents, although the sizes of the currents may be reduced. Third, bacTMEM175s also produce K^+ conductance when expressed in mammalian cells, which are less likely to have endogenous proteins to associate with them. Fourth, the animal and bacterial TMEM175 homologs differ in sequences and selectivity; although all are K^+-selective, hTMEM175 is more selective for Cs^+ than K^+ and bacTMEM175s is more selective for K^+ than Cs^+. Since ion selectivity is generally determined by the pore-forming proteins, the simplest interpretation of these data is that TMEM175 is a pore-forming subunit of K_{EL}. Studying the single-molecule behaviors of K_{EL} will require single-channel recording from lysosomes expressing TMEM175, but such recordings have not so far been successful.

How does K_{EL} achieve its K^+ selectivity without a GYG/GFG-containing P loop? Between eukaryotic K_{EL}s and their bacterial homologs, the regions with significant sequence similarity are S1 and S2 (Figure S4). Since both channels are selective for K^+, it is tempting to speculate that K_{EL}'s K^+-selective pore is formed by the first transmembrane-spanning segment. Similarly, uses of both P-loop-based and P-loop-independent mechanisms to achieve ion selectivity are found in other channels. For example, the voltage-activated Ca^{2+} channels (Ca_Vs) and the Ca^{2+}-release-activated Ca^{2+} channels (CRAC) are both selective for Ca^{2+}, but they use distinct pore structures. In Ca_V, the glutamate-containing selectivity filter is formed by four P loops, each contributed from one of the four repeats (Tang et al., 2014; Yang et al., 1993). In CRAC, the central pore is aligned by TM1s from multiple ORAI protein subunits; the glutamate residues at the extracellular end of TM1s, one from each subunit, form a "glutamate ring" as the ion selectivity filter (Hou et al., 2012). If TMEM175's IS1 and IIS1 indeed form the ion filter, the negatively charged residues (D/E) within the helices could potentially interact with K^+ to achieve the K^+ selectivity (Figure S2A). To elucidate the detailed selectivity and permeation mechanism of K_{EL} at the atomic level requires detailed mutagenesis studies and high-resolution structural information.

With the identification of the major K^+ conductance, how lysosomes control $\Delta\Psi$ is now much better understood. Our patch-clamp recordings revealed K^+, Na^+, Cl^-, and H^+ conductances (Cang et al., 2014). The organelle is highly permeable to H^+ (P_H/P_K: ~7,000 in macrophages). Because of the high $[H^+]$ in the lumen (~0.03 mM at pH4.5 to 0.01 mM at pH5.0), the H^+ permeability makes large contribution to $\Delta\Psi$ ($(P_H/P_K)[H^+]_{lumen}$ = ~70 mM to 210 mM). The Cl^- and H^+ conductance is likely due to the CLC H^+/Cl^- transporters/channels (Graves et al., 2008; Stauber and Jentsch, 2013) and, for H^+, many other channels that are also permeable to H^+. Native lysosomal Ca^{2+} currents are small or undetectable (data not shown); the ion's contribution to $\Delta\Psi$ is perhaps mainly through its regulation of other conductances. For the Ca^{2+} permeability, Ca_V proteins normally found on the plasma membrane are also functional in lysosomes (Tian et al., 2015). In addition, overexpressing several ion channels such as TRPMLs and P2X4 generates lysosomal Ca^{2+}-permeable channels and leads to Ca^{2+} release (Dong et al., 2010; Huang et al., 2014; LaPlante et al., 2004). At

Figure 7. TMEM175 Forms the Native K_{EL}, Controls $\Delta\Psi$, Contributes to Lysosomal pH Stability, and Regulates Organelle Fusion during Autophagy

(A) Targeted disruption of mouse TMEM175 (mTMEM175) gene in RAW264.7 mouse macrophage cells using CRISPR. The sequences of WT in the IS2-encoding region (amino acid sequences shown) are in red, followed by the PAM sequences (TGG, in blue). Three mutations (two deletions and one insertion) detected in the KO cells are aligned against the WT.

(B–E) (B–D) Representative lysosomal currents recorded using voltage-clamping from a control (B), a knockout (KO; C), and a knockout cell transfected with hTMEM175 (KO + hTMEM175) (D). Averaged current amplitudes at +100 mV are in (E). Recordings were done using a ramp protocol (−100 mV to +100 mV in 1 s, Vh = 0) with 150 mM NMDG in the pipettes and 150 mM K^+ (or NMDG, as indicated) in the bath.

(F–H) Representative (F and G) lysosomal membrane potentials $\Delta\Psi$ recorded using current-clamping (I = 0) from a control (F) and a KO (G) RAW264.7 cell with varying bath $[K^+]$ as indicated. Averaged $\Delta\Psi$ values are in (H).

(I–K) Lysosomal pH from control (I and K) and KO (J and K) RAW264.7 cell lysosomes before and after starvation. pH value distribution histograms (fitted to Gaussian functions) are in (I) and (J), and averaged values are in (K).

(L and M) Autophagosome-lysosome fusion as assayed with the mCherry- and GFP-tagged LC3 (tandem tag, illustrated) transfected into control (WT), KO cells, or KO cells co-transfected with hTMEM175, with or without bafilomycin (bafi) treatments. (L) Cells were starved for 2 hr and imaged for RFP (top panels, indicative of total number of autophagosome puncta before and after phagosome-lysosome fusion) and GFP (middle, indicative of autophagosome before fused with lysosome, due to low GFP activity in acidic organelles) puncta. RFP and GFP signals are merged in the bottom panels. Scale bar, 10 μm. (M) Averaged numbers of GFP and RFP puncta upon treatments as indicated (n = 20–50).

(N) Numbers of GFP-positive puncta normalized to those of RFP-positive ones.

Data are presented as mean ± SEM. See also Figure S5.

"rest," lysosomes have much lower P_{Na} than P_K as estimated by patch-clamp recordings from enlarged lysosomes (P_{Na}/P_K, ~0.3) (Cang et al., 2014) and by indirect measurements with semi-intact lysosomes (Casey et al., 1978; Henning, 1975). As such, the "resting" membrane potential is perhaps largely determined by H^+ and K^+ permeabilities and is predicted to be ~−18 mV at pH5.0 and +12 mV at pH4.5 (assuming 140 mM $[K^+]_{cyt}$. P_{Cl}/P_K is small [< 0.1 in macrophages; data not shown]). These predicted values are within the range of those measured with current clamp using artificially enlarged lysosomes (~> 0 mV) and those estimated with a FRET-based "non-invasive" method using semi-intact lysosomes (−19 mV) (Koivusalo et al., 2011). Upon electrical and chemical stimulation such as decrease in $[ATP]_{cyt}$, luminal alkalinization, and/or increases in PI(3,5)P2 concentration, lysosomes can exhibit an ~30-fold increase in P_{Na}/P_K. At the "stimulated" state, Na^+ and K^+ permeabilities are expected to be major determinants of $\Delta\Psi$. Indeed, Na^+ conductance-dependent long depolarizations with properties resembling those of action potentials have been observed in a subset of lysosomes (Cang et al., 2014). There are two Na^+ selective channels, the voltage-independent TPC2 and, in some cells such as cardiac myocytes, the depolarization- and alkalinization-activated TPC1 (Cang et al., 2013, 2014; Wang et al., 2012). Consistent with the idea that TPCs are the major Na^+ conductance, $\Delta\Psi$ in lysosomes deficient in TPCs is insensitive to changes in $[Na^+]$ (Cang et al., 2013). Unlike plasma membrane, the organelle membrane appears to exhibit only one major type of K^+ channels. Knocking out K_{EL} largely eliminated the total organelle K^+ conductance and $\Delta\Psi$'s K^+ sensitivity. Such simplicity in K^+ conductance can perhaps be explained by the relatively similar environment organelles face across different cell types.

The roles of lysosomal $\Delta\Psi$ are still not well established, but they may include several cellular functions. First, $\Delta\Psi$ regulates organelle pH. The pumping of H^+ into the lumen by the vacuolar H^+ pump (V-ATPase) to achieve acidic pH leads to a highly negative $\Delta\Psi$ (lumen more positive), in turn limiting the H^+ pumping ability of the V-ATPase due to increased proton motive force, unless the high $\Delta\Psi$ is dissipated by influx of anions and/or efflux of cations. Cl^-, Na^+, and K^+ can each serve as a $\Delta\Psi$-dissipating counterion when $\Delta\Psi$ is more hyperpolarized than the ion's equilibrium potential and if lysosome is permeable to the ion (Mindell, 2012; Steinberg et al., 2010). The ion channels mediating the counterion permeability are not well established. Knocking out CFTR Cl^- channels or ClC Cl^-/H^+ exchangers/channels has moderate effect on lysosomal pH (Steinberg et al., 2010) (but see Graves et al. [2008]). Knocking out TPCs (Cang et al., 2013) or K_{EL} leads to luminal alkalinization during nutrient starvation. In nutrient-replete cells, however, alkalinization in the mutants is minimal, suggesting that there is redundancy in the ion conductance mechanism. Future studies using cells with multiple major ion channel genes simultaneously disrupted will reveal the genetic redundancy.

Second, $\Delta\Psi$ may regulate substance digestion, via its influence on luminal pH, and the subsequent substance export from lysosomes. Consistent with this idea, lysosomes without functional TPCs have lower export rates for charged amino acids (Cang et al., 2013). Third, $\Delta\Psi$ may regulate Ca^{2+} release from lysosomes. Lysosomes have ~0.5 mM luminal Ca^{2+} (Christensen et al., 2002; Churchill and Galione, 2001). Hyperpolarizing $\Delta\Psi$ can increase Ca^{2+} release from voltage-independent Ca^{2+}-permeable channels such as TRPs and P2X4 (Huang et al., 2014; Xu and Ren, 2015). Hypothetically, depolarizing $\Delta\Psi$ can also activate lysosomal Ca^{2+} release from Ca_Vs (Tian et al., 2015). Finally, $\Delta\Psi$ may influence the insertion of membrane proteins with charged residues and regulate the fusion between organelles, either directly by acting on charged lipids and protein residues or indirectly by stimulating Ca^{2+} release to promote organelle fusion. Among mitochondria, the homotypic organelle fusion requires inner membrane $\Delta\Psi$; increased K^+ permeability with K^+ ionophore valinomycin suppresses such fusion (Meeusen et al., 2004). In K_{EL} knockout cells, the fusion between lysosomes and autophagosomes appears to be accelerated. Lysosomes also fuse with other organelles such as endosomes and with plasma membrane. Future studies with in vitro assays will directly test the contribution of ion channels and $\Delta\Psi$ to organelle trafficking and inter-organelle interaction.

In summary, we have identified TMEM175 as a new K^+ channel that is responsible for the K^+ conductance K_{EL} in endosomes and lysosomes. The molecular mechanisms underlying the major ion permeability in lysosomes are now understood. Mutations in lysosomal Cl^-/H^+, Ca^{2+}, or Na^+ channel/transporter genes in human patients and in mice have been found to cause lysosomal pH instability, reduced amino acid export, compromised metabolic response and physical endurance, neuronal degeneration, lysosomal storage diseases, fatty liver disease, osteopetrosis, and resistance to Ebola viral infection (Grimm et al., 2014; Sakurai et al., 2015; Stauber and Jentsch, 2013; Sun et al., 2000; Xu and Ren, 2015). K_{EL} is a major ionic transport channel in the lysosomal membrane and it conducts the most abundant ion inside the cell. Future studies with mutant animal models will reveal the organismal function of lysosomal K^+ permeability in health and diseases.

EXPERIMENTAL PROCEDURES

Cell Culture and cDNA Transfection

Cells were cultured at 37°C in a humidified CO_2 (5%) incubator. Details for cell culture and cDNAs used for transfection are described in the Supplemental Experimental Procedures.

CRISPR Knockout and shRNA Knockdown

To knock out mTMEM175 in RAW264.7 cells, sequence *GAGCAGGCAGTGGATTCCGA* was targeted using the lentiCRISPRv2 vector. Details for CRISPR knockout and shRNA knockdown are described in the Supplemental Experimental Procedures.

Protein Chemistry and Protein Localization

For the western blot used in Figure 3, a polyclonal TMEM175 antibody (Proteintech Group, Cat. 19925-1-AP) was used at 1:500 for western blot analysis. Western blot and protein localization are described in the Supplemental Experimental Procedures.

Lysosome pH Imaging and Autophagosome-Lysosome Fusion Assay

Lysosome pH measurement and autophagosome-lysosome fusion imaging were described previously (Cang et al., 2013) and are described in detail in the Supplemental Experimental Procedures.

Electrophysiology

Electrophysiology using enlarged organelles followed previously described methods (Saito et al., 2007). Endosomes were enlarged by transfecting the Rab5 mutant Rab5-Q79L (Stenmark et al., 1994) (a gift from Roger Chang). Lysosomes were enlarged by treatment with 1 μM (RAW264.7 cells, HEK293T cells, cardiac myocytes, and fibroblasts) or 5 μM (neurons and glia) vacuolin-1 for 1–6 hr (RAW264.7) or overnight (HEK293T cells, neurons, glia, cardiac myocytes, and fibroblasts) (Cerny et al., 2004; Dong et al., 2010). Individual organelles were manually released from each cell sliced open with a glass pipette. Recordings were performed with a Multiclamp 700B amplifier and a Digidata 1440A data acquisition system controlled by PClamp software (Molecular Device).

Unless otherwise indicated, the bath solution used in organelle voltage-clamp recordings contained (in mM) 145 K-methanesulfonate, 5 KCl, 10 HEPES (pH 7.2). The pipette solution contained (in mM) 145 K-methanesulfonate, 5 KCl, 10 MES (pH 5.5). For current clamp recordings presented in Figures 1 and 7, the bath solution contained (in mM) 140 K-methanesulfonate (or substituted with NMDG- methanesulfonate), 10 NaOH, 2 $MgCl_2$, 1 EGTA, 0.39 $CaCl_2$, 10 HEPES, (pH 7.2) by methanesulfonic acid. Pipette solution contained (in mM) 70 KCl, 70 NaCl, 2 $CaCl_2$, 1 $MgCl_2$, 10 HEPES, 10 MES, 10 glucose, (pH 5.5) by NaOH. Liquid junction potentials were corrected online.

For the recordings described in Figure 2 for screening purposes, the pipette solution contained (in mM) 70 KCl, 70 NaOH, 2 $CaCl_2$, 1 $MgCl_2$, 10 HEPES, 10 MES, 10 glucose, 2× amino acids, (pH 4.6) by methanesulfonic acid. For the recordings of LCTC1-6, 8, and 9, the bath solution contained (in mM) 145 K-methanesulfonate, 5 KCl, 0.39 $CaCl_2$, 1 EGTA, 10 HEPES, (pH 7.2) by NMDG. For the recordings of control and LCTC7, 10-16, bath solution contained (in mM) 50 KCl, 100 NaOH, 2 $MgCl_2$, 0.39 $CaCl_2$, 1 EGTA, 10 HEPES, (pH 7.2) by methanesulfonic acid.

The relative permeability of hTMEM175 was obtained with endosomal recordings under bi-ionic conditions. The pipette solution contained (in mM) 150 KOH, 5 HCl, 10 MES, (pH 5.5) by methanesulfonic acid. The bath solutions contained (in mM) 150 NaOH (or 150 CsOH, 100 $Ca(OH)_2$), 5 HCl, 10 HEPES, (pH 7.2) by methanesulfonic acid. Relative permeabilities were calculated using the following equations:

$$P_K/P_X = [X]_{cytosol}\ \exp(\Psi_{rev}F/RT)\Big/[K]_{lumen},\ (X = Na \text{ or } Cs)$$

$$P_{Ca}/P_K = \left\{[K]_{lumen}\exp(-\Psi_{rev}F/RT)[\exp(-\Psi_{rev}F/RT)+1]\right\}\Big/\left\{4[Ca]_{cytosol}\right\},$$

where P_K, P_{Na}, P_{Ca} are the permeabilities to K^+, Na^+, and Ca^{2+}, respectively, Ψ_{rev} is the measured reversal potential, F is Faraday's constant, R is the gas constant, and T is the absolute temperature.

The inhibition curves presented in Figures S3E and S3F were fitted with the Hill equation:

$$I/I_0 = 1\Big/\left[1+(X/IC_{50})^h\right],$$

where I and I_0 are the currents obtained in the presence and absence of inhibitors, respectively, X is the inhibitor concentration, IC_{50} is the concentration required for half-maximal inhibition, and h is the Hill coefficient.

For whole-cell recordings of bacTMEM175s (Figures 6 and S4), the bath solution consisted of (in mM) 150 KOH, 10 TEA, 3 HCl, 1 $MgCl_2$, 1 $CaCl_2$, 10 HEPES, (pH 7.2) by methanesulfonic acid. Pipette solution contained (in mM) 150 KOH, 5 HCl, 0.1 $CaCl_2$, 10 HEPES, (pH 7.2) by methanesulfonic acid.

Data Analysis

Data were analyzed using Clampfit, OriginPro, Prism, and Excel. Numeric data were shown as mean ± SEM. Statistical significance was calculated with t test.

SUPPLEMENTAL INFORMATION

Supplemental Information includes Supplemental Experimental Procedures and five figures and can be found with this article online at http://dx.doi.org/10.1016/j.cell.2015.08.002.

AUTHOR CONTRIBUTIONS

D.R. and C.C. conceived the project. C.C. performed patch-clamp recording and autophagosome-lysosome fusion assay. K.A. contributed Figure 3. Y.-j.S performed pH imaging. K.A., D.R., and B.G. developed reagents. D.R. and C.C. wrote the paper. All authors reviewed the manuscript.

ACKNOWLEDGMENTS

We thank Drs. Sora Lee, Carol Deutsch, and David Clapham for suggestions; Robert Edwards and Roger Chang for the use of Rab5-Q79L; Drs. Haijun Chen and Mickey Marks for reagents; and Dr. Bin Wu for pilot studies. This work was supported, in part, by funding from NIH, the University of Pennsylvania Research Foundation (to D.R.), the Centre National de la Recherche Scientifique (to B.G.), and the Basic Science Research Program (through the National Research Foundation of Korea funded by the Ministry of Education (number 2012R1A6A3A03040071 to Y.-j.S.).

Received: April 10, 2015
Revised: June 10, 2015
Accepted: July 13, 2015
Published: August 27, 2015

REFERENCES

Accardi, A., and Miller, C. (2004). Secondary active transport mediated by a prokaryotic homologue of ClC Cl- channels. Nature *427*, 803–807.

Bertl, A., Blumwald, E., Coronado, R., Eisenberg, R., Findlay, G., Gradmann, D., Hille, B., Köhler, K., Kolb, H.-A., MacRobbie, E., et al. (1992). Electrical measurements on endomembranes. Science *258*, 873–874.

Cang, C., Zhou, Y., Navarro, B., Seo, Y.-J., Aranda, K., Shi, L., Battaglia-Hsu, S., Nissim, I., Clapham, D.E., and Ren, D. (2013). mTOR regulates lysosomal ATP-sensitive two-pore Na(+) channels to adapt to metabolic state. Cell *152*, 778–790.

Cang, C., Bekele, B., and Ren, D. (2014). The voltage-gated sodium channel TPC1 confers endolysosomal excitability. Nat. Chem. Biol. *10*, 463–469.

Casey, R.P., Hollemans, M., and Tager, J.M. (1978). The permeability of the lysosomal membrane to small ions. Biochim. Biophys. Acta *508*, 15–26.

Cerny, J., Feng, Y., Yu, A., Miyake, K., Borgonovo, B., Klumperman, J., Meldolesi, J., McNeil, P.L., and Kirchhausen, T. (2004). The small chemical vacuolin-1 inhibits Ca(2+)-dependent lysosomal exocytosis but not cell resealing. EMBO Rep. *5*, 883–888.

Chapel, A., Kieffer-Jaquinod, S., Sagné, C., Verdon, Q., Ivaldi, C., Mellal, M., Thirion, J., Jadot, M., Bruley, C., Garin, J., et al. (2013). An extended proteome map of the lysosomal membrane reveals novel potential transporters. Mol. Cell. Proteomics *12*, 1572–1588.

Christensen, K.A., Myers, J.T., and Swanson, J.A. (2002). pH-dependent regulation of lysosomal calcium in macrophages. J. Cell Sci. *115*, 599–607.

Churchill, G.C., and Galione, A. (2001). NAADP induces Ca2+ oscillations via a two-pool mechanism by priming IP3- and cADPR-sensitive Ca2+ stores. EMBO J. *20*, 2666–2671.

Dong, X.P., Shen, D., Wang, X., Dawson, T., Li, X., Zhang, Q., Cheng, X., Zhang, Y., Weisman, L.S., Delling, M., and Xu, H. (2010). PI(3,5)P(2) controls membrane trafficking by direct activation of mucolipin Ca(2+) release channels in the endolysosome. Nat. Commun. *1*, 38.

Doyle, D.A., Morais Cabral, J., Pfuetzner, R.A., Kuo, A., Gulbis, J.M., Cohen, S.L., Chait, B.T., and MacKinnon, R. (1998). The structure of the potassium channel: molecular basis of K+ conduction and selectivity. Science *280*, 69–77.

Goldstein, S.A., Bockenhauer, D., O'Kelly, I., and Zilberberg, N. (2001). Potassium leak channels and the KCNK family of two-P-domain subunits. Nat. Rev. Neurosci. *2*, 175–184.

Graves, A.R., Curran, P.K., Smith, C.L., and Mindell, J.A. (2008). The Cl-/H+ antiporter ClC-7 is the primary chloride permeation pathway in lysosomes. Nature *453*, 788–792.

Grimm, C., Holdt, L.M., Chen, C.C., Hassan, S., Müller, C., Jörs, S., Cuny, H., Kissing, S., Schröder, B., Butz, E., et al. (2014). High susceptibility to fatty liver disease in two-pore channel 2-deficient mice. Nat. Commun. *5*, 4699.

Haggie, P.M., and Verkman, A.S. (2009). Defective organellar acidification as a cause of cystic fibrosis lung disease: reexamination of a recurring hypothesis. Am. J. Physiol. Lung Cell. Mol. Physiol. *296*, L859–L867.

Heginbotham, L., Lu, Z., Abramson, T., and MacKinnon, R. (1994). Mutations in the K+ channel signature sequence. Biophys. J. *66*, 1061–1067.

Henning, R. (1975). pH gradient across the lysosomal membrane generated by selective cation permeability and Donnan equilibrium. Biochim. Biophys. Acta *401*, 307–316.

Hille, B. (2001). Ion Channels of Excitable Membranes, Third Edition (Sinauer Associates).

Honoré, E. (2007). The neuronal background K2P channels: focus on TREK1. Nat. Rev. Neurosci. *8*, 251–261.

Hou, X., Pedi, L., Diver, M.M., and Long, S.B. (2012). Crystal structure of the calcium release-activated calcium channel Orai. Science *338*, 1308–1313.

Huang, X., and Jan, L.Y. (2014). Targeting potassium channels in cancer. J. Cell Biol. *206*, 151–162.

Huang, P., Zou, Y., Zhong, X.Z., Cao, Q., Zhao, K., Zhu, M.X., Murrell-Lagnado, R., and Dong, X.P. (2014). P2X4 forms functional ATP-activated cation channels on lysosomal membranes regulated by luminal pH. J. Biol. Chem. *289*, 17658–17667.

Jiang, Y., Lee, A., Chen, J., Ruta, V., Cadene, M., Chait, B.T., and MacKinnon, R. (2003). X-ray structure of a voltage-dependent K+ channel. Nature *423*, 33–41.

Klionsky, D.J., Abdalla, F.C., Abeliovich, H., Abraham, R.T., Acevedo-Arozena, A., Adeli, K., Agholme, L., Agnello, M., Agostinis, P., Aguirre-Ghiso, J.A., et al. (2012). Guidelines for the use and interpretation of assays for monitoring autophagy. Autophagy *8*, 445–544.

Koivusalo, M., Steinberg, B.E., Mason, D., and Grinstein, S. (2011). In situ measurement of the electrical potential across the lysosomal membrane using FRET. Traffic *12*, 972–982.

Krapivinsky, G., Medina, I., Eng, L., Krapivinsky, L., Yang, Y., and Clapham, D.E. (1998). A novel inward rectifier K+ channel with unique pore properties. Neuron *20*, 995–1005.

LaPlante, J.M., Ye, C.P., Quinn, S.J., Goldin, E., Brown, E.M., Slaugenhaupt, S.A., and Vassilev, P.M. (2004). Functional links between mucolipin-1 and Ca2+-dependent membrane trafficking in mucolipidosis IV. Biochem. Biophys. Res. Commun. *322*, 1384–1391.

MacKinnon, R., and Miller, C. (1989). Mutant potassium channels with altered binding of charybdotoxin, a pore-blocking peptide inhibitor. Science *245*, 1382–1385.

Meeusen, S., McCaffery, J.M., and Nunnari, J. (2004). Mitochondrial fusion intermediates revealed in vitro. Science *305*, 1747–1752.

Miller, C. (1995). The charybdotoxin family of K+ channel-blocking peptides. Neuron *15*, 5–10.

Mindell, J.A. (2012). Lysosomal acidification mechanisms. Annu. Rev. Physiol. *74*, 69–86.

Mizushima, N., and Komatsu, M. (2011). Autophagy: renovation of cells and tissues. Cell *147*, 728–741.

Nichols, C.G., and Lopatin, A.N. (1997). Inward rectifier potassium channels. Annu. Rev. Physiol. *59*, 171–191.

Nugent, T., and Jones, D.T. (2012). Detecting pore-lining regions in transmembrane protein sequences. BMC Bioinformatics *13*, 169.

Saito, M., Hanson, P.I., and Schlesinger, P. (2007). Luminal chloride-dependent activation of endosome calcium channels: patch clamp study of enlarged endosomes. J. Biol. Chem. *282*, 27327–27333.

Sakurai, Y., Kolokoltsov, A.A., Chen, C.C., Tidwell, M.W., Bauta, W.E., Klugbauer, N., Grimm, C., Wahl-Schott, C., Biel, M., and Davey, R.A. (2015). Ebola virus. Two-pore channels control Ebola virus host cell entry and are drug targets for disease treatment. Science *347*, 995–998.

Schröder, B., Wrocklage, C., Pan, C., Jäger, R., Kösters, B., Schäfer, H., Elsässer, H.P., Mann, M., and Hasilik, A. (2007). Integral and associated lysosomal membrane proteins. Traffic *8*, 1676–1686.

Stauber, T., and Jentsch, T.J. (2013). Chloride in vesicular trafficking and function. Annu. Rev. Physiol. *75*, 453–477.

Steinberg, B.E., Huynh, K.K., Brodovitch, A., Jabs, S., Stauber, T., Jentsch, T.J., and Grinstein, S. (2010). A cation counterflux supports lysosomal acidification. J. Cell Biol. *189*, 1171–1186.

Stenmark, H., Parton, R.G., Steele-Mortimer, O., Lütcke, A., Gruenberg, J., and Zerial, M. (1994). Inhibition of rab5 GTPase activity stimulates membrane fusion in endocytosis. EMBO J. *13*, 1287–1296.

Sun, M., Goldin, E., Stahl, S., Falardeau, J.L., Kennedy, J.C., Acierno, J.S., Jr., Bove, C., Kaneski, C.R., Nagle, J., Bromley, M.C., et al. (2000). Mucolipidosis type IV is caused by mutations in a gene encoding a novel transient receptor potential channel. Hum. Mol. Genet. *9*, 2471–2478.

Tang, L., Gamal El-Din, T.M., Payandeh, J., Martinez, G.Q., Heard, T.M., Scheuer, T., Zheng, N., and Catterall, W.A. (2014). Structural basis for Ca2+ selectivity of a voltage-gated calcium channel. Nature *505*, 56–61.

Tian, X., Gala, U., Zhang, Y., Shang, W., Nagarkar Jaiswal, S., di Ronza, A., Jaiswal, M., Yamamoto, S., Sandoval, H., Duraine, L., et al. (2015). A voltage-gated calcium channel regulates lysosomal fusion with endosomes and autophagosomes and is required for neuronal homeostasis. PLoS Biol. *13*, e1002103.

Tusnády, G.E., and Simon, I. (2001). The HMMTOP transmembrane topology prediction server. Bioinformatics *17*, 849–850.

Wang, X., Zhang, X., Dong, X.P., Samie, M., Li, X., Cheng, X., Goschka, A., Shen, D., Zhou, Y., Harlow, J., et al. (2012). TPC proteins are phosphoinositide-activated sodium-selective ion channels in endosomes and lysosomes. Cell *151*, 372–383.

Xu, H., and Ren, D. (2015). Lysosomal physiology. Annu. Rev. Physiol. *77*, 57–80.

Yang, J., Ellinor, P.T., Sather, W.A., Zhang, J.F., and Tsien, R.W. (1993). Molecular determinants of Ca2+ selectivity and ion permeation in L-type Ca2+ channels. Nature *366*, 158–161.

Yellen, G., Jurman, M.E., Abramson, T., and MacKinnon, R. (1991). Mutations affecting internal TEA blockade identify the probable pore-forming region of a K+ channel. Science *251*, 939–942.

Zhu, M.X., Ma, J., Parrington, J., Calcraft, P.J., Galione, A., and Evans, A.M. (2010). Calcium signaling via two-pore channels: local or global, that is the question. Am. J. Physiol. Cell Physiol. *298*, C430–C441.

Zweifach, A., and Lewis, R.S. (1993). Mitogen-regulated Ca2+ current of T lymphocytes is activated by depletion of intracellular Ca2+ stores. Proc. Natl. Acad. Sci. USA *90*, 6295–6299.